Generation of cytocompatible superhydrophobic Zr–Cu–Ag metallic glass coatings with antifouling properties for medical textiles

Materials Today Bio 12 (2021) 100148

Contents lists available at ScienceDirect

Materials Today Bio

journal homepage: www.journals.elsevier.com/materials-today-bio

Generation of cytocompatible superhydrophobic Zr–Cu–Ag metallic glass coatings with antifouling properties for medical textiles

Elham Sharifikolouei [a,*], Ziba Najmi [b], Andrea Cochis [b], Alessandro Calogero Scalia [b], Maryam Aliabadi [c], Sergio Perero [a], Lia Rimondini [b]

[a] Department of Applied Science and Technology, Politecnico di Torino, Corso Duca Degli Abruzzi 24, 10129, Turin, TO, Italy
[b] Department of Health Sciences, Center for Translational Research on Autoimmune and Allergic Diseases – CAAD, Università Del Piemonte Orientale UPO, Corso Trieste 15/A, 28100, Novara, NO, Italy
[c] Competence Center Textile Chemistry, Environment, Energy, German Institute of Textile and Fiber Research, 73770, Denkendorf, Germany

ARTICLE INFO

Keywords:
Metallic glass
Coating
Superhydrophobic
Antifouling
Antibacterial textile

ABSTRACT

Zirconium–Copper-based metallic glass thin films represent promising coatings in the biomedical sector for their combination of antibacterial property and wear resistance. However, finding a Zr–Cu metallic glass composition with desirable cytocompatibility and antibacterial property is extremely challenging. In this work, we have created a cytocompatible and (super-)hydrophobic Zr–Cu–Ag metallic glass coating with ≈95% antifouling properties. First, a range of different chemical compositions were prepared via Physical Vapor Deposition magnetron by co-sputtering Zr, Cu, and Ag onto a Polybutylene terephthalate (PBT) substrate among which $Zr_{93.5}Cu_{6.2}Ag_{0.2}$, $Zr_{76.7}Cu_{22.7}Ag_{0.5}$, and $Zr_{69.3}Cu_{30.1}Ag_{0.6}$ were selected to be further investigate for their surface properties, antibacterial activity, and cytocompatibility. Scanning electron microscopy (SEM) images revealed a micro-roughness fibrous structure holding superhydrophobic properties demonstrated by specimens' static and dynamic contact angle measurements ranging from 130° to 150°. The dynamic contact angle measurements have shown hysteresis below 10° for all coated samples which indicated the superhydrophobicity of the samples. To distinguish between antifouling and bactericidal effect of the coating, ions release from coatings into Luria Bertani Broth (LB), and Dulbecco's Modified Eagle Medium (DMEM) solutions were evaluated by inductively coupled plasma mass spectrometry (ICP-MS) measurements after 24 h and 5 days. Antifouling properties were evaluated by infecting the specimens' surface with the Gram-positive *Staphylococcus aureus* and the Gram-negative *Escherichia coli* strain reporting a ≈95% reduction of bacteria adhesion as visually confirmed by FESEM and fluorescent live/dead staining. Human mesenchymal stem cells (hMSC) were used for direct cytocompatibility evaluation of coated samples and their metabolic activity was evaluated via relative fluorescence unit after 24 h and 5 days confirming that it was comparable to the controls (>97% viable cells). The results were further visualized by FESEM, fluorescent staining by Live/Dead Viability/Cytotoxicity Kit and confirmed the cytocompatibility of all coated samples. Finally, hMSC′ cytoplasm was stained by May Grunwald and Giemsa after 5days to detect and visualize the released ions which have diffused through the cells' membrane.

1. Introduction

Healthcare-associated infections (HCAI), also referred to nosocomial infections are major cause of health-care complications leading to prolonged hospitalization, long-term disabilities, and unnecessary deaths [1]. A recent survey from European Center for Disease Prevention and Control estimated a total of 8.9 million healthcare-associated infections to occur each year in European hospitals and long-term care facilities. The fiber-based textile materials are popular choices and are widely used in health-care sector because of the variety of advantages they offer such as their light weight, low cost, flexibility in shape, and washing without corrosion, and therefore, they are indispensable. Surgical gowns, nurse aprons, bedding, mask, curtains are only some examples of instances which avoid the spread of hazardous viruses and bacteria for both medical teams and patients. Textiles in the medical or health-care sectors are often contaminated by pathogenic microorganisms mainly by smear contamination (in particular by contact with the hands) or by droplets and aerosols (droplet nuclei) released when coughing, sneezing or

* Corresponding author.
E-mail address: elham.sharifikolouei@polito.it (E. Sharifikolouei).

https://doi.org/10.1016/j.mtbio.2021.100148
Received 14 July 2021; Received in revised form 6 October 2021; Accepted 8 October 2021
Available online 26 October 2021

speaking. Pathogens can remain active on textile surfaces for days to months, consequently, they could be an additional source of cross-transmission from person to person [2]. In this context, development of textile surfaces that inhibit the adhesion and as a consequence the proliferation and spread of pathogenic germs is crucial to minimize the spread of multidrug-resistant germs in hospital and high-risk environments.

Bacteria vary in size, shape, surface characteristics, morphology, metabolism, development, and adaptation to changes in their surrounding environments. Bacteria with various physicochemical characteristics show diverse responses against the different antimicrobial materials; in fact, for a given materials surface, each bacterium adhere differently [3]. In other words, depending on the bacteria's surface characteristics which are defined by its genome, adhering bacteria might have a preference to adhere on hydrophobic or hydrophilic surfaces. It is demonstrated that germs with hydrophobic surface would adhere better on hydrophobic surfaces while germs with hydrophilic properties adhere better on polar surfaces. Therefore, many scientists have focused on the development of various antimicrobial textile materials following the modification of their surface properties such as chemistry, energy, wettability, roughness and charge. Ellinas et al. [4] has shown that bacteria adhesion to superhydrophobic surfaces remains low and stable over time and even without further treatments could reduce the bacterial biofilm formation. Imani et al. [5]. has developed a flexible plastic wrap with hierarchical structures which was the outcome of combining micro- and nano-structuring including a fluorosilane treatment for enhancing their hydrophobicity and oleophobicity. The processed surfaces have demonstrated the omniphobic properties repelling liquids with various surface tensions by reducing biofilm formation with the efficiency of 87% and 84% for methicillin-resistant *Staphylococcus aureus* and *Pseudomonas aeruginosa*, respectively. In another work by Ma et al. [6]. a novel zeolitic imidazolate framework 8@thiolated graphene composites-based polyimide (PI) nanofibrous membrane (ZIF 8@GSH/PI) was developed and fabricated via a facile electrospinning and in situ hydrothermal synthesis approaches. The synergetic properties of ZIF 8, GSH, nanoscale roughness, and hierarchical structure have led to the antibacterial activity of the membranes against *Bacillus subtilis* and *Escherichia coli*. These results emphasize on the role of surface topography (roughness) as a fundamental parameter to control the hydrophilicity/hydrophobicity of the materials which eventually determines the surface wettability, germ repellency, and germ adhesion. Development of hydrophobic and superhydrophobic surfaces is of interest for other applications as well (e.g. water purification) and therefore, the state of the art for the development of superhydrophobic polymeric textiles could be utilized for generation of antifouling textiles as well [7–10].

Another suitable approach is the functionalization of the surface by exploiting antibacterial agents such as silver (Ag) and copper (Cu) [11]. Ag has broad-spectrum antibacterial activities and good inhibitory effects on both Gram-positive and Gram-negative bacteria [12,13]. Ferraris et al. [14] has also used this approach to generate Ag-nanocluster coatings with excellent antibacterial properties. Cu is also frequently used based on its antibacterial contact-killing due to release of ions. Contact with copper surface has been shown to damage the integrity of bacterial membrane through different mechanisms: it can directly damage bacterial proteins as well as induce the formation of hydroxyl radicals, leading to cell damage through interaction with the cell DNA, enzyme and other proteins [15].

Metallic glasses are a revolutionary class of materials where crystallization upon solidification is suppressed, keeping them in the disordered state. The absence of a crystalline structure is the reason for their extraordinary properties over traditional crystalline alloys [16]. In the biomedical industry, Zr-based BMG are popular choices for their good (bio-)corrosion resistance. To enhance their antibacterial properties, some researchers have focused on surface energy and surface microstructure modification of Zr-based BMG mechanically or via electrochemical or chemical etching processes to prepare superhydrophobic surfaces which acts as antifouling surfaces [17] [–] [19]. Similarly, employing a nanostructured geometry of the surface such as nanospike, nanoblade, or nanodart is another strategy to develop bactericidal properties on the surface [20]. In this phenomenon, the nanospike or nanostructure penetrates and damages the bacteria membrane. This mechanism is known as "mechano-bactericidal". However, it has been recently found that if efficient number of antibacterial elements such as Ag or Cu are present in the chemical composition of the material, they can show antibacterial properties with no further treatment of surface modifications. This is a very different scenario in comparison to the use of Ag or Cu in the form of nanoparticles because Ag and Cu in metallic glasses appear in the form of randomly distributed atoms within the matrix. However, the difficulty associated with fabrication of bulk metallic glasses has pushed their application in the form of thin film. In particular, zirconium (Zr)-based metallic glass thin films has been reported for their promising antibacterial properties and cytocompatibility combined with their corrosion resistance in body fluids. For example, antibacterial properties are reported by Y. Lui et al. [21], and by G.I. Nkou Bouala et al. [22] for $Zr_{38}Cu_{36}Al_{18}Ag_8$, and $Zr_{73}Cu_{16}Ag_{11}$ metallic glasses, respectively. The other advantage of metallic glass coatings (thin films) for antibacterial properties is their better mechanical properties in comparison with other popular coating choices such as diamondlike carbon (DLC). In fact, DLC is of interest due to its chemically inertness and compatibility with human cells but it is quite brittle, and it requires expensive high-temperature processing. Metallic glass coating, on the other hand, is compatible with human cells, has better ductility and can be processed by inexpensive low-temperature processes such as sputtering techniques [23].

Metallic glass formation is extremely sensitive to chemical composition. Therefore, in the current study, metallic glass coatings based on Zr and Cu with small addition of Ag is prepared via Physical Vapor Deposition (PVD) magnetron co-sputtering on Polybutylene terephthalate (PBT) substrate, using a physical mask to create discrete areas with different compositions due to the fact that each discrete unmasked area has a different distance with respect to each sputtering target (Zr, Cu, Ag). To develop the antibacterial (antifouling) properties, in the current work, we are relying on the one-step sputtering process of Zr–Cu–Ag metallic glass on PBT without the further need to mechanically or chemically modifying the surface structure. Our choice of textile is PBT which is a member of polyester family of polymers and therefore is well investigated. In fact, it has very similar chemical composition as well as properties to those of Polyetylene terephthalate (PET) which has been previously approved as a cytocompatible polymer and has wide range of biomedical applications including sutures, heart valves, surgical meshes, scaffolds, urinary and bloodstream catheters [24,25]. Compared to PET, PBT has strength and stiffness but has higher impact strength and similar chemical resistance. Regarding its mechanical properties, PBT can reach up to 15% elongation and its tensile strength is in the order of 38 MPa. Since it crystallizes more rapidly than PET, PBT is a preferred choice for injection molding in the industry [26,27]. In this work, metallic glass coated PBTs were firstly characterized for their surface morphology by SEM, and their chemical composition was confirmed by EDS. Samples were investigated for their surface characteristics measuring the contact angles of deionized water, Luria Bertani Broth (LB), and Dulbecco's Modified Eagle Medium (DMEM) on the samples 'surfaces via sessile-drop method and Ellipse-fitting. Samples were then infected with the pathogen *Staphylococcus aureus* to test their antifouling properties. Finally, specimens cytocompatibility was verified by cultivating human mesenchymal stem cells (BhMSC) directly onto their surface.

2. Materials and methods

2.1. Materials preparation

As-prepared melt-blown Polybutylene terephthalate (PBT, provided by DITF, Denkendorf, Germany) was co-sputtered (RF and DC power

supply) to deposit Zr–Cu–Ag coatings. Silver (Sigma-Aldrich 99.999%), Zr (NanoVision s.r.l. 99.99%) and Copper (NanoVision s.r.l. 99.99%) targets were used to deposit the coatings. The three cathodes are confocal and point the extraction cone on the center of the sample holder. The distance between each cathode and the substrate surface is 24.5 cm, while the centers of the circular targets are 14 cm apart from each other, and they are placed on a hypothetical 9 cm radius circumference. Each area of the substrate receives difference part of the extracted atom flux from each target, leading to different final composition. The pressure before deposition was 10^{-5} Pa, in the deposition chamber. The working pressure/atmosphere was pure argon at $10^{-2}/10^{-1}$ Pa, dynamically maintained. The power over target were 35 W in RF for copper (Cu); 15 W in RF for silver (Ag); 300 W in DC for zirconium (Zr) to form a coating of 1 μm thickness. The choice of using RF for conducting materials like copper and silver is to reduce the deposition rate of these metals and having hence better control on the amount of the deposited materials, being their deposition rate higher with respect to the zirconium one. The deposition time was 1 h. To be able to simultaneously deposit number of different chemical compositions, a physical mask was placed on top of the substrate (PBT) with discrete hole areas. Each hole had a different distance to the targets (Zr, Cu, Ag), leading to the generation of a range of compositions on PBT substrate. Each discrete area was further cut and investigated for its properties. Out of all prepared samples, three compositions were selected for further investigation of their antifouling properties and cytocompatibility.

2.2. Physical-chemical characterization

2.2.1. SEM-EDS, and XRD analysis

Surface morphology and chemical composition of as-prepared melt blown PBT substrate and sputtered samples were investigated by scanning electron microscopy (SEM) equipped with energy dispersive spectroscopy (EDS, JCM - 6000Plus Versatile Benchtop JEOL, for compositional assessment). Small angle X-Ray scattering was conducted using a Panalytical Empyrean X-ray diffractometer with Cu Kα radiation ($\lambda = 1.54$ Å) with a step size of 0.001°. Field emission scanning electron microcopy (FESEM) was used to investigate the samples after antibacterial and cytotoxicity tests (FESEM, ZEISS SUPRA TM 40).

2.2.2. Static and dynamic contact angle measurement

The static contact angle between the samples surfaces and the liquids were measured by sessile-drop method and Ellipse-fitting using the drop contour analysis system (OCA 200, Dataphysics, Germany). Deionized water, Luria Bertani Broth (LB, Sigma-Aldrich), and Dulbecco's Modified Eagle Medium (DMEM, Sigma-Aldrich) were utilized as liquid mediums. Liquid drop of a known volume (2–3 μl) was generated at the tip of the needle (needle outer diameter = 0.4 mm) and then was gently seeded onto the surface. The static contact angle was measured when the drop was standing on the surface and the three-phase boundary was not moving. Dynamic contact angle measurements were performed by adjusting the needle near the surface of the sample. Deionized water droplet (2–3 μl) was dosed in order to moistens the sample. While the needle was still in the middle of droplet, its volume was started to expand with a dosing rate of 1 μl s^{-1}. A steady state value of the contact angle at the growing state was defined as the advancing contact angle. Subsequently, the receding contact angle was measured by reducing the drop volume at the same rate. In our Experiments, the temperature, density, and dynamic viscosity of water during the measurement have been recorded as follow: T = 22.5 °C, $\rho_w = 998$ kg m^{-3}, and $\mu_w = 0.9$ mPas, respectively. The contact angles have been measured at the three different positions on each prepared sample in order to confirm the homogeneity of their surface.

2.2.3. Ions release evaluation

Specimens (4 × 4 mm^2 square) were submerged with 7 ml/specimen of Luria Bertani (LB, Sigma-Aldrich) or Dulbecco's Modified Eagle Medium (DMEM, Sigma-Aldrich) solutions and were placed inside a shaker (120 rpm, T = 37 °C) for 1, and 5 consequent days. At each time points the supernatants were collected and used to investigate the functionalization ion-release (Zr, Cu, Ag) from the surface using inductively coupled plasma mass spectrometry (ICP-MS, iCAP Q, ThermoFischer).

2.3. Antibacterial evaluation

2.3.1. Strain growth condition

Bacteria were purchased from the American Type Culture Collection (ATCC, Manassas, USA). Specimens' antibacterial properties were assayed towards the methicillin/oxacillin (MRSA) resistant *Staphylococcus aureus* strain (Gram-positive, ATCC 43300) and *Escherichia coli* (Gram-negative, ATCC 25922). Bacteria were cultivated in Trypticase Soy agar plates (TSA, Sigma-Aldrich) and incubated at 37 °C until round single colonies were formed; then, few colonies were collected and spotted into 15 ml of LB broth (Sigma-Aldrich) and incubated overnight at 37 °C under agitation (120 rpm). The day after a fresh broth culture was prepared prior to the experiment by diluting bacteria into fresh medium till a final concentration of 1×10^5 bacteria/ml corresponding to an optical density of 0.001 at 600 nm wavelength using a spectrophotometer [28] (Spark, from Tecan, Switzerland).

2.3.2. Direct antibacterial activity evaluation

Antibacterial properties were assayed after 90 min (early time point) and 24 h (late time point) of direct infection. Accordingly, 50 μl of LB medium containing a known 1×10^5 bacteria number were directly drop-seeded onto specimens' surface (4 × 4 mm^2 square) and incubated at 37 °C; at each timepoint the supernatants were gently collected from each specimen to evaluate the number of viable floating bacteria whereas adhered bacteria were detached from specimens' surface by vortex (30 s each, 3 times). and sonication (5 min each, 3 times). The number of viable bacteria was determined by the colony forming unit count (CFU) as previously detailed [29], the metabolic activity of the adhered bacteria was further evaluated by the colorimetric metabolic assay alamar blue (alamarBlue™, ready-to-use solution from Life Technologies) by directly adding the dye solution (0.0015% in phosphate buffer saline) onto the infected specimens; after 4 h incubation in the dark the fluorescent signals (expressed as relative fluorescent units – RFU) were detected at 590 nm by spectrophotometer (Spark, from Tecan, Switzerland). Moreover, the fluorescent Live/Dead assay (BacLight™, Bacterial Viability Kit for microscopy, Invitrogen) was applied to visually detect viable colonies adhered to the fibers; images were collected by confocal microscopy (Leica TCS SP8 confocal laser scanning microscope, Leica Microsystems). Finally, Field emission electron microscopy (FESEM, SUPRATM 40, Zeiss) imaging was used to detect biofilm-like colonies aggregates; briefly, specimens were dehydrated by the alcohol scale (70-80-90-100% ethanol, 1 h each), swelled with hexamethyldisilazane, mounted onto stubs with conductive carbon tape and covered with a chromium layer.

2.3.3. Not direct antibacterial evaluation

In order to evaluate a possible antibacterial effect of the released ions, specimens (4 × 4 mm^2 square) were submerged with 7 ml of LB broth and maintained at 37 °C inside a shaker (120 rpm) for 1, 5 days, following the same procedure exploited for the ions release evaluation (section 2.2.3). At each time point the supernatants were collected and used to cultivate bacteria at a defined concentration (1×10^5 cells/ml); bacteria cultivated with supernatants obtained from ions-free PBT were considered as control. The released ions killing activity was evaluated in terms of metabolic

activity that was measured by the alamar blue assay as previously detailed.

2.4. In vitro cytocompatibility evaluation

2.4.1. Cells cultivation

Human bone marrow-derived mesenchymal stem cells (BhMSC) were purchased from PromoCell (C-12974) and cultivated in low-glucose DMEM (Sigma-Aldrich) supplemented with 15% fetal bovine serum (FBS, Sigma-Aldrich) and 1% antibiotics at 37 °C, 5% CO_2 atmosphere. Cells were cultivated until 80%–90% confluence, detached by a trypsin-EDTA solution (0.25% in PBS), harvested and used for Experiments.

2.4.2. Direct contact evaluation

Cells were directly seeded onto specimens' surface (4 × 4 mm^2 square) at a defined density (2 × 10^4 cells/sample) and cultivated for 24 h allowing adhesion and spread. Then, the cells viability was evaluated by means of metabolic activity using the metabolic colorimetric alamar blue assay as prior described; then, to estimate the exact number of viable adhered cells, they were detached from specimens' surface by trypsin, counted by the trypan blue using a Burker chamber and seeded into a new polystyrene plate. After 6 h adhesion into the new plate, the fluorescent Live/Dead assay was applied to visually check for viable cells (Live/Dead, Viability/Cytotoxicity Kit for mammalian cells, Invitrogen); images were collected with a digital EVOS FLoid microscope (from Life Technologies). Finally, the morphology of cells aligned following fibers orientation was visually investigated by FESEM imaging as prior detailed.

2.4.3. Not direct contact evaluation

In order to evaluate a possible toxic effect of the released ions, specimens (4 × 4 mm^2 square) were submerged with 7 ml of DMEM medium and maintained at 37 °C inside a shaker (120 rpm) for 1, and 5 days. At each time point the supernatants were collected and used to cultivate cells seeded at a defined concentration (2 × 10^4 cells/well) into multiwell plates; cells cultivated with supernatants obtained from ions-free PBT were considered as control. The released ions potential toxic effect was evaluated in terms of metabolic activity by means of the alamar blue assay as previously detailed. Moreover, ions internalization and accumulation were histologically evaluated by using the May-Grünwald-Giemsa staining as described in previous literature [30].

2.5. Statistical analysis of data

Experiments were performed in triplicate. Results were statistically analyzed using the SPSS software (v.20.0, IBM, USA). First, data normal distribution and homogeneity of variance were confirmed by the Shapiro-Wilk's and the Levene's test, respectively; then, groups were compared by the one-way ANOVA using the Tukey's test as post-hoc analysis. Significant differences were established at $p < 0.05$.

3. Results and discussion

3.1. Physical-chemical properties evaluation

Sputtered samples with a range of different chemical compositions were prepared through co-sputtering Zr–Cu–Ag on PBT substrate, using a physical mask to divide each sample. This approach enables us to prepare samples with slightly different chemical compositions which is an important aspect when it comes to Zr–Cu based metallic glass thin film properties. The relative chemical composition of each sample (the surface not covered by the physical mask) is controlled by the respective distance of the sample area from each of the targets (Zr, Cu, Ag). EDS analysis was conducted on the samples to confirm their exact chemical composition. The chemical composition of the selected samples (MG1, MG2, MG3) is presented in Table 1.

Table 1
Chemical composition of deposited coatings onto PBT substrate.

Sample	Zr (at%)	Cu (at%)	Ag (at%)
MG1	93.57 (±1.02)	6.22 (±1.02)	0.20 (±0.12)
MG2	76.73 (±0.47)	22.71 (±0.32)	0.56 (±0.15)
MG3	69.30 (±0.41)	30.10 (±0.20)	0.60 (±0.19)

Fig. 1A shows the schematic representation of this process, and how the sample appears to naked eyes. Fig. 1B shows the SEM image of the PBT structure. (Since PBT is sputtered by Zr, Cu, Ag, to avoid repetition, the SEM images of samples after sputtering are presented in Fig. S1 in supplementary materials). The SEM picture shows a highly porous fibrous structure in which some fibers perturbed into the surface and have created a micro-rough surface. All prepared samples were investigated for static water contact angle measurements via sessile drop method, presented in Fig. 1C. Samples show contact angles ranging approximately between 130° to 150°, indicating hydrophobic to superhydrophobic surface properties. Previous contact angle measurements from Zr–Cu based metallic glasses have been reported values between 90° to 110°, indicating hydrophobic surfaces [31,32]. The excessive hydrophobicity of our samples could be explained based on the observed highly porous fibrous structure in SEM because of the presence of entrapped air bubbles inside porous structure [33]. This assumption is even further reinforced due to the observation of free-standing water droplets on sample surfaces held upside down (see Fig. S2 in supplementary materials). Furthermore, the micro-roughness introduced by the randomly distributed fibers on the surface, could be another contributor to the hydrophobicity of the samples. Among the prepared samples, three samples from three different regions of the chemical composition range with different contact angles were selected to be further investigated for their antifouling properties (Fig. 1C, indicated by the green box).

Selected samples were further investigated for the confirmation of amorphous structure via low angle X-ray scattering, shown in Fig. 2. The lack of sharp peaks and the broad hump in their x-ray spectra confirms the formation of amorphous structure for the generated thin films. After confirming for the successful formation of Zr–Cu based metallic glass coatings, selected samples were investigated further for their wetting behavior in contact with other mediums. Since the antibacterial tests were conducted in Luria Bertani broth (LB) medium, and cytocompatibility test were conducted in Dulbecco's Modified Eagle Medium (DMEM), the sessile drop contact angle measurement was repeated for each sample using LB and DMEM. Fig. 3 shows the static contact angle (CA) measurements of these mediums on PBT and coated samples (MG1, MG2, MG3). Going first to the water contact angles, it can be concluded that both non-sputtered sample (PBT), and sputtered samples are all hydrophobic. It should be noted that during contact angle measurements, the first generated volume of water (when water droplets are still held by the needle due to their surface tension) on the surface could not be measured because of the liquids' minimal tendency to wet the surface. Based on the results, the hydrophobicity of samples has generally increased after sputtering. In particular, hydrophobicity of non-sputtered PBT (CA = 124.5(±0.3)°) surface increases to form superhydrophobic surface in MG3 (CA = 150.8(±0.1)°). Similar trend of increasing contact angle is observed when LB and DMEM were used as a medium. Even though, there are small differences among these values, they are all indicating hydrophobic to superhydrophobic properties for all samples. Therefore, one can conclude that the samples are all hydrophobic regardless of the type of liquid medium.

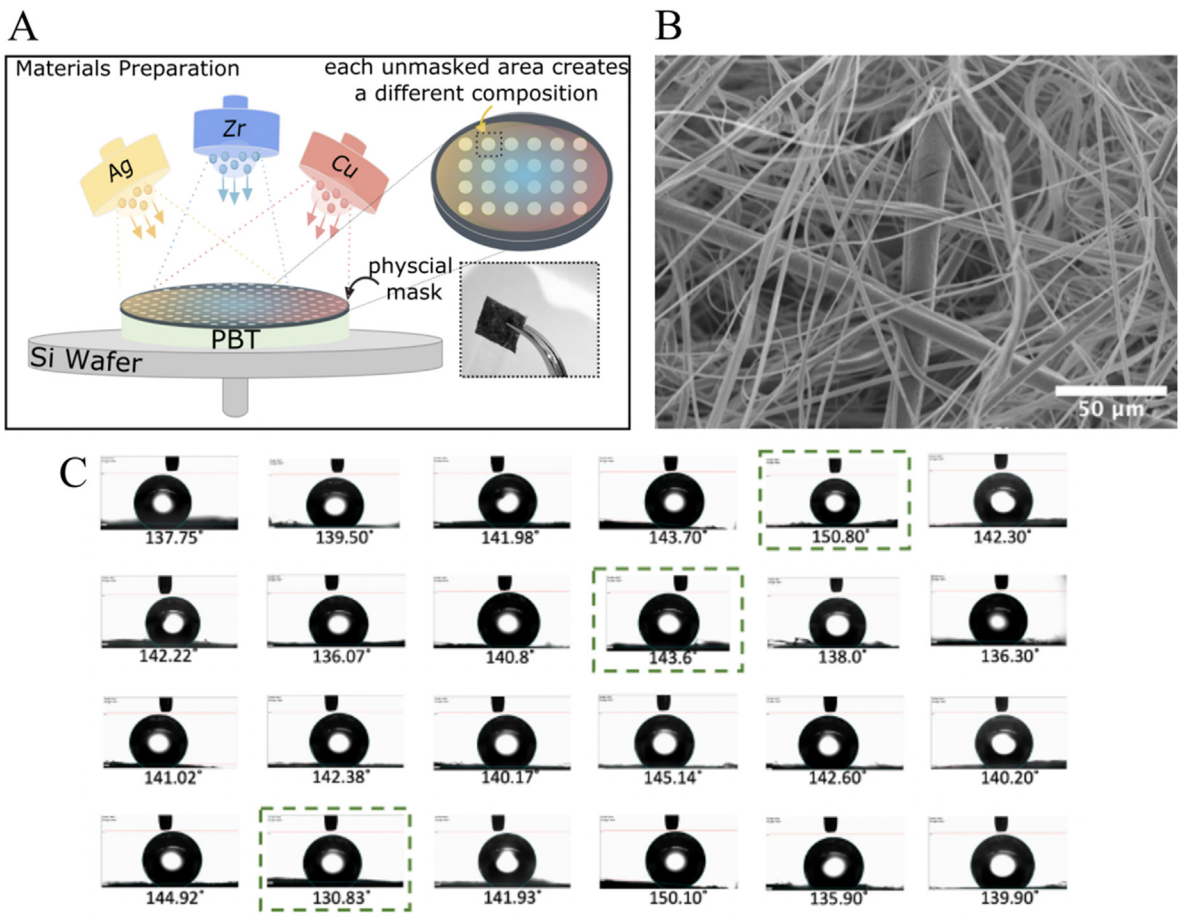

Fig. 1. (A) Schematic representation of the co-sputtering process: the physical mask with discrete holes is placed on top of PBT substrate. The color gradient represents the chemical composition gradient (B) SEM image of PBT (C) Sessile drop static contact angle measurement of deionized water on PBT surface after sputtering Zr, Cu, Ag. The selected samples for further antifouling properties investigation are marked by the green box. The complete list of measured values is presented in Table S1 is supplementary materials.

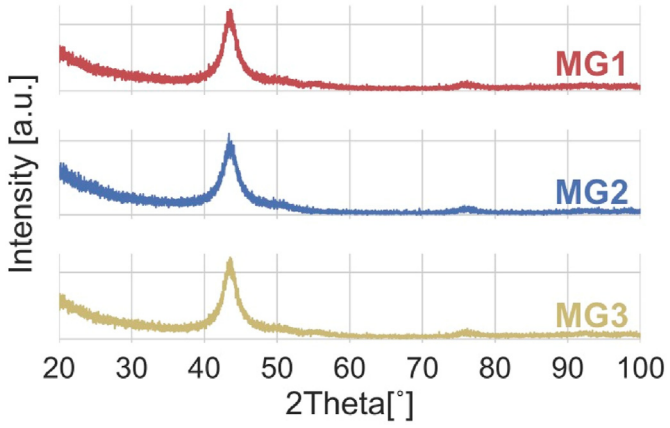

Fig. 2. Small angle X-Ray scattering conducted on the sputtered samples MG1, MG2, and MG3. The broad peak confirms the formation of Zr–Cu based metallic glass coatings.

To investigate the contact angle hysteresis, dynamic contact angle measurements were performed on samples' surface. Table 2 reports the values for advancing and receding angles of water droplets on samples surfaces and their hysteresis values (the difference between advancing and receding angle) and it is compared with their static contact angle values. The full videos of dynamic contact angle measurements could be found in supplementary materials. According to this table, all sputtered samples show hysteresis lower than 10°. This would mean that in fact, all sputtered samples have superhydrophobic surfaces. Among sputtered samples, MG3 has the lowest hysteresis value (3.5). The hysteresis value for non-sputtered sample, PBT is about 15°.

To distinguish between antifouling and bactericidal effect of the coating, samples were immersed inside LB and DMEM (7 ml/each) for a period of 1 day and 5 days at 37 °C and under agitation (100 rpm) to fasten the ion-release process. The concentration of released ions was measured by Inductively coupled plasma mass spectrometry (ICP-MS). ICP-MS measurements are shown in Fig. 4. Results demonstrates that even though the major component of the coating is Zr (above 69 atom%), it is the Cu ions that has the maximum release from all samples. These results were predictable considering the wear resistance of Zr in contrast to Cu. The highest Zr ion release after 5 days in DMEM belongs to MG1, with the highest Zr at% of 93.57 ± 1.02 among all samples whereas the highest Cu ion release after 5 days belongs to MG3 with the highest Cu at % in its composition (30.10 ± 0.20). Since Ag concentration in all three samples is below 0.6 at%, it was expected to have minimal Ag ion release into mediums. Therefore, it is no surprise to detect almost no Ag ions in the medium.

3.2. Antibacterial activity

3.2.1. Direct evaluation

In this study, besides of *Escherichia coli, Staphylococcus aureus* was selected as a suitable candidate for the investigation of antibacterial properties since it is one of the major causes of hospital acquired

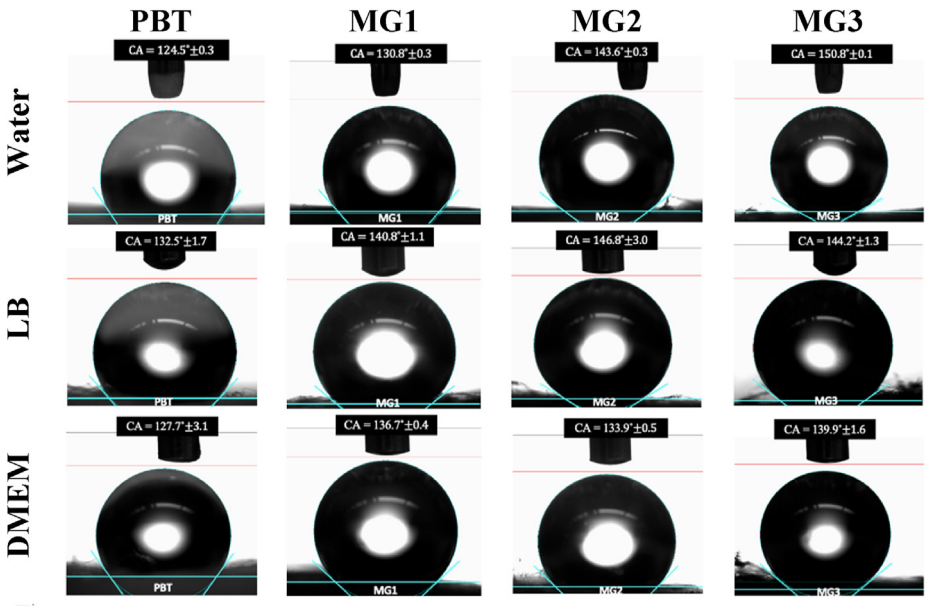

Fig. 3. Sessile drop contact angle measurement on samples using water, LB, and DMEM.

Table 2
Static vs dynamic contact angle measurements of water droplets on non-sputtered sample (PBT) and sputtered samples (MG1, MG2, MG3). Dynamic angles are reported as Advancing and Receding angles.

Samples	Contact Angle [°]			
	Static	Advancing	Receding	Hysteresis
PBT	124.5(±0.3)	135.4(±0.2)	120.1(±1.1)	15.3
MG1	130.8(±0.3)	135.1(±0.9)	127.4(±1.0)	7.7
MG2	143.5(±0.3)	146.1(±1.3)	138.9(±2.5)	7.2
MG3	150.7(±0.1)	153.9(±0.2)	150.4(±1.5)	3.5

infection and has high ability of resistance to commonly used antibiotics [34]. The main aim of this part was to assess whether the specimens hold antifouling properties due to their superhydrophobic surface highlighted by the contact angles or an antibacterial killing activity thanks to the released ions as prior showed in the ICP assay. Therefore, bacteria number and metabolism were checked not only onto specimens' surface (direct assay) but also within the supernatants (not direct assay). Moreover, an early (90 min) time point representative for the adhesion process [35] was planned, as well as a second late time point (24 h) was considered to monitor bacteria proliferation over time. The results relative to the direct evaluation are reported in Fig. 5.

Fig. 5A shows Live/Dead images of *S.aureus* and *E.coli* after 90 min of direct contact with the specimens' surfaces. This figure confirms that only few colonies were adhered to the sputtered surfaces in comparison to the PBT control but that such colonies were mostly alive (stained in green) (Live/Dead pictures after 24 h are presented in Fig. S3 in supplementary materials). Fig. 5B depicts the metabolic activity of *S.aureus* and *E.coli* in the same test (90 min-direct contact) where non-sputtered sample (PBT) was considered as control (viability = 100%). The differences between bacterial viability after 90 min are very minimal for all three samples. The metabolic activity of *E.coli* after 90 min is significantly reduced for all three samples ($p < 0.05$ indicated by *) while the metabolic activity of *S. aureus* after 90 min is higher than that of *E.coli* but is still significantly reduced for MG2 and MG3 ($p < 0.05$ indicated by *). For each type of bacteria, the difference in metabolic activity among all three samples is very minimal. These results suggest the efficacy of the coating in the reduction of bacteria metabolic activity.

Fig. 5C shows the metabolic activity of *S.aureus* and *E.coli* after 24 h. The metabolic activity of *S.aureus* after 24 h is approximately 15% increased compared to 90 min time point for all sputtered samples and their value is almost the same for all three samples. However, the metabolic activity of *E.coli* after 24 h is almost identical to the 90 min time point for MG3 while its value is significantly increased for MG1 and MG2. The increases in bacteria metabolic activity suggests an antifouling activity rather than bactericidal properties.

FESEM images were obtained from these samples after 90 min and 24 h of direct contact with *S.aureus* and *E.coli*. Fig. 6. Shows the FESEM images of *S.aureus* on samples surfaces after 90 min and 24 h it demonstrates low infections for all samples. However, MG3 appears to have the lowest amount of infection. The difference among PBT and coated samples is more significantly visible when looking at the FESEM images after

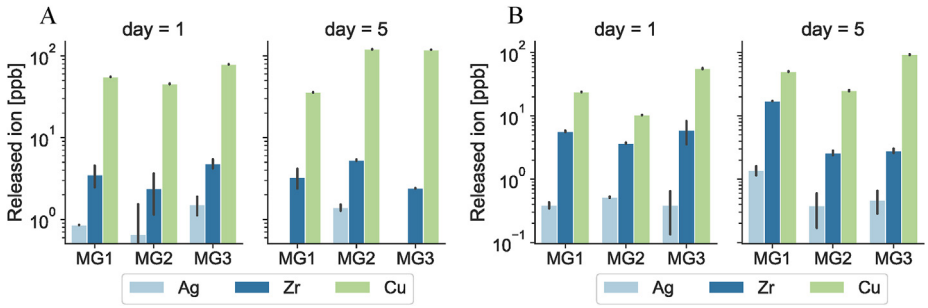

Fig. 4. Ions release profile of specimens submerged with (A) LB and (B) DMEM after 1day (left panels) or 5 days (right panels) immersion at 37 °C. Cu resulted as the prevalent ion released in the supernatant by reaching >100 ppb after 5 days in both LB and DMEM media.

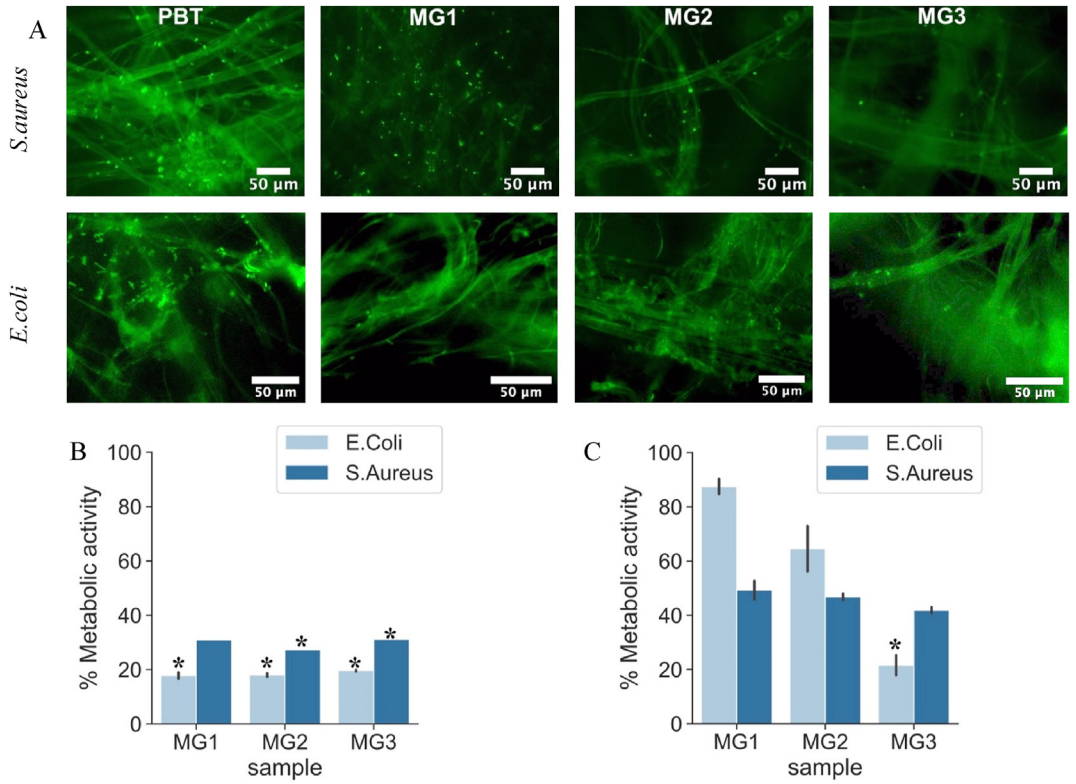

Fig. 5. Direct antibacterial test to assess antiadhesion and anti-bacterial properties of PBT coated by Zr–Cu–Ag metallic glass: A) Live/Dead assay of S.aureus and E.coli on the surface after 90 min incubation time B) Metabolic activity of *S. aureus* and E.coli on samples' surface after 90 min. Uncoated PBT is used as a control and was considered to have 100% viability C) Metabolic activity of *S. aureus* and E.coli on samples' surface after 24 h. Uncoated PBT is used as a control and was considered to have 100% viability.

24 h. It is clear that only PBT specimens were colonized by biofilm-like aggregates even though MG1-MG2-MG3 sputtered surfaces presented some random single colonies with an apparently living morphology (round and intact).

Similarly, FESEM images of *E.coli* on samples surfaces after 90 min and 24 h are shown in Fig. 7. The infections for all samples after 90 min are very minimal. After 24 h, the difference among samples is much more significant. As expected, the non-sputtered sample, PBT has biofilm-like aggregates. MG1 appears to have significant number of colonized bacteria as well. This was already expected based on metabolic activity of *E.coli* reported in Fig. 5C. MG3 appears to have the minimum number of colonized *E.coli* on its surface. This could be justified based on its superhydrophobic surface with the static contact angle of 150.7°(±1) and the dynamic contact angle hysteresis of 3.5.

As a significant confirmation of the antifouling hypothesis, the CFU count was performed by detaching adhered colonies after both 90 min and 24 h. Results are summarized in Table 3. Considering that specimens were infected with the known bacterial concentration of 1×10^5 cells/specimen, after 90 min, $>$ 95% of the applied colonies were prevented to adhere (highest value reported is 1×10^3 for MG1). However, after 24 h all the specimens reached an infection rate in the 10^5 power, thus displaying a remarkable increase of the viable adhered colonies. So, the CFU count gave a confirmation of the hypothesized antifouling activity ascribable to the sputtered specimens due to their superhydrophobic properties.

In fact, from both static and dynamic contact angle measurement, it was shown that MG3 surface shows superhydrophobic properties (static CA = 150.7°(±0.1), and hysteresis = 3.5°). Considering the *S. aureus* hydrophilic surface, it is no surprising that its attachment on our superhydrophobic surfaces face significant difficulty. The reduced bacterial adhesion on superhydrophobic surfaces was found to result from the reduced protein adsorption and the entrapped air layer between the LB droplet (containing bacteria cells) and the surface [33,36]. The presence of entrapped air layer was also observed when holding bacterial droplet upside down on the samples. Bacterial adhesion is mediated by different types of interactions which can be nonspecific or specific. It is generally considered that proteins tend to adsorb more favorably onto surfaces with contact angles of 60°–95° [37]. However, superhydrophobic surfaces have been found to have low protein adsorption and easy protein detachment thus resulting in a low bacterial adhesion. The later was called as Lotus effect introduced in 1997 to explain the self-cleaning property of the Lotus leaf [38]. On superhydrophobic surface, air is entrapped in most of the surface area, hence significantly reducing the contact area between water and sample surface as well as between the bacteria cells and the sample surface. Therefore, the adhesion of bacteria cells to sample surface is much weak and when the water droplet rolls off from sample surfaces, bacteria cells are taken away [36]. Furthermore, the bacterial suspension medium is LB which we have previously shown that its contact angles with the sputtered samples are between 140° and 144°, meaning for the bacteria to have low chance of attaching due to the minimum surface contact available. However, as we have observed from the results, the sputtered surfaces are not capable of total prohibition of bacterial attachment. The reason for such attachment might be related to the surface morphology of samples. Considering the high surface roughness and the varying porosity of fibrous structure on samples surfaces, there is a chance that bacteria start adhering to the more porous area of the surface and proliferate from those seeds. Furthermore, the CFU analysis of *S. aureus* and *E. coli* after 90 min and

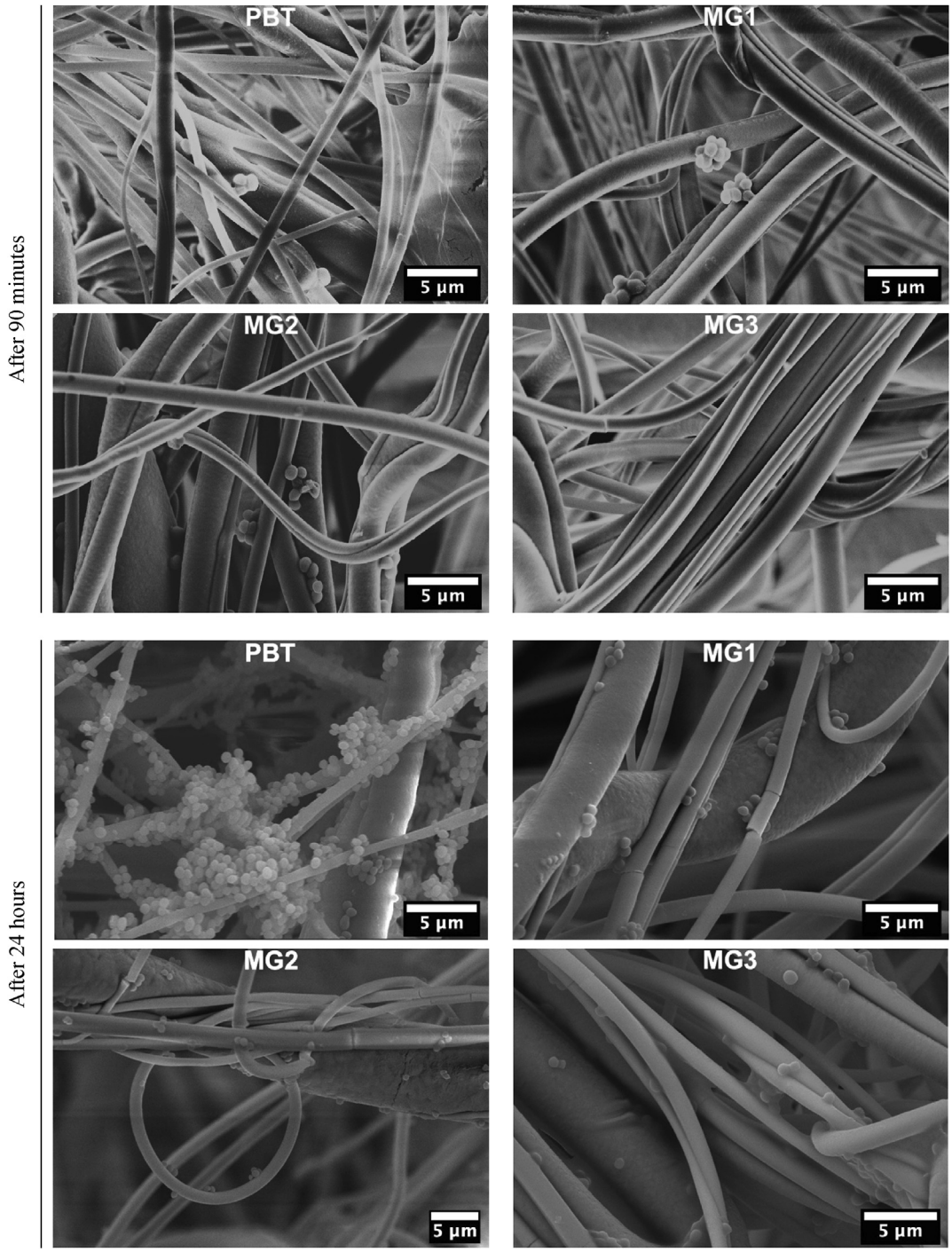

Fig. 6. FESEM images of non-sputtered (PBT) sample and sputtered PBT by Zr–Cu–Ag metallic glass coatings(MG1, MG2, MG3) after 90 min and 24 h of direct contact to *S. aureus*.

24 h presented in Table 3 shows that the number of living bacteria attached to samples' surfaces for *S. aureus* were about 4.44x (in serial dilution of 10^2) and 2.1x (in serial dilution of 10^5) less than that of the non-sputtered sample (PBT) after 90 min and 24 h respectively. The same trend was observed for *E.coli.* The number of living *E. coli* attached to the samples' surfaces after 90 min and 24 h indicated the reduction of 54.6x (in serial dilution of 10^2) and 9x (in serial dilution of 10^5) in adherence respectively, in comparison with the non-sputtered sample (PBT). These results were further visually confirmed by Live/Dead staining after 90 min of incubation time. These pictures show the same trend for the number of alive bacteria for the samples. The untreated PBT appears to have the maximum number of live bacteria, while MG3, among sputtered samples, has the lowest number of live bacteria (the Live/Dead images after 24 h incubation time are presented in Fig. S3. the supplementary materials) which could be related to its chemical composition (highest Cu at% among all samples). Higher resolution pictures of samples surface after antibacterial test were obtained using FESEM where images after 24 h incubation (Figs. 6 and 7), clearly show the significant reduction in the number of bacteria attached to the samples surface. While biofilm-like colonies aggregates are formed on non-sputtered sample (PBT), all three coated samples show reduced numbers and scattered bacteria on the surface. This is an important aspect in prevention of

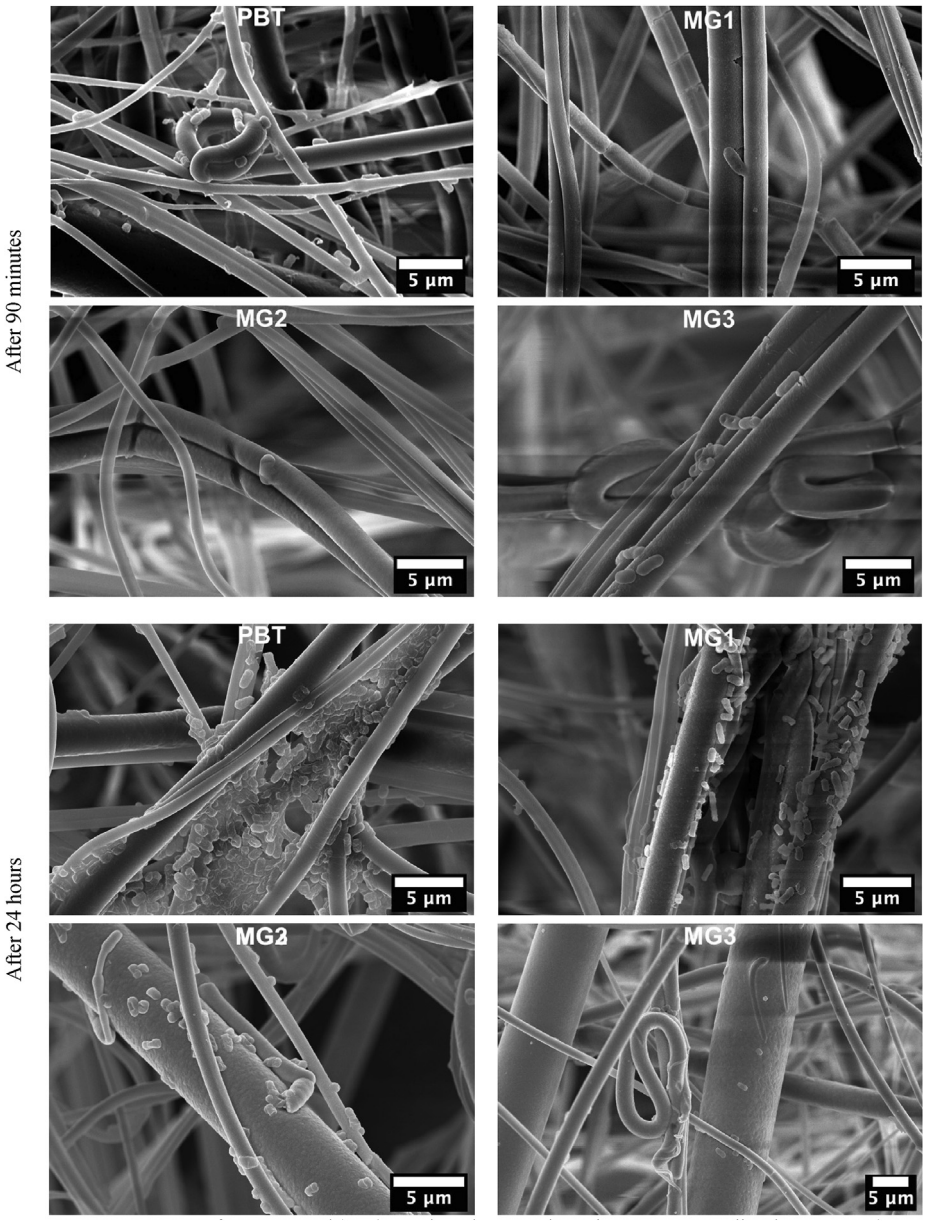

Fig. 7. FESEM images of non-sputtered (PBT) sample and sputtered PBT by Zr–Cu–Ag metallic glass coatings(MG1, MG2, MG3) after 90 min and 24 h of direct contact to E.coli.

Table 3
Number of viable colonies (CFU) of S.aureus and E.coli attached to the sample surface after 90 min and 24 h of infection.

Samples	Adhered CFU count			
	After 90 min ($x10^2$)		After 24 h ($x10^5$)	
	S.aureus	*E.coli*	*S.aureus*	*E.coli*
PBT	40 (±2)	71(±3)	9.5 (±2)	15(±2)
MG1	10 (±1)	1(±0)	5 (±1)	3(±1)
MG2	8 (±1)	1(±0)	4 (±1)	2(±1)
MG3	9 (±3)	2(±1)	4.5 (±1)	0(±0)

bacterial infection since the formation of clump is the first step in the formation of biological membrane leading to biofilm formation leading to the development of drug-resistance mechanisms.

These findings are in line with previous investigations suggesting that superhydrophobic surfaces are successful in the prevention of bacterial adhesion. Crick et al. [34], reported significant reduction of *E. coli* attachment (79% reduction versus uncoated glass) and *S. aureus* (58% reduction relative to uncoated glass) after 1 h submersion of silicone elastomer thin film in bacterial suspension. It has been argued that the reduction of bacterial attachment was connected to the super-hydrophobic properties of samples' surface, limiting the contact between the aqueous bacteria suspension and the elastomers' grooves. Similarly, Privet et al. [39], showed reduction of *S. aureus* adhesion to the silica-colloid-doped fluorinated substrates down to 2.08 logarithms in comparison to untreated samples.

3.2.2. Not direct evaluation

After completing the direct evaluation suggesting for a specimens' antifouling activity, the potential toxic effect of the sputtered ions was evaluated by a not direct assay where ions release was conducted into LB medium by incubating specimens for 1 and 5 days. Afterwards, super-natants containing the released ions were collected and used to cultivated bacteria which metabolic activity was assayed to verify their viability. Results are reported in Fig. 8. In general, bacteria metabolic activity was

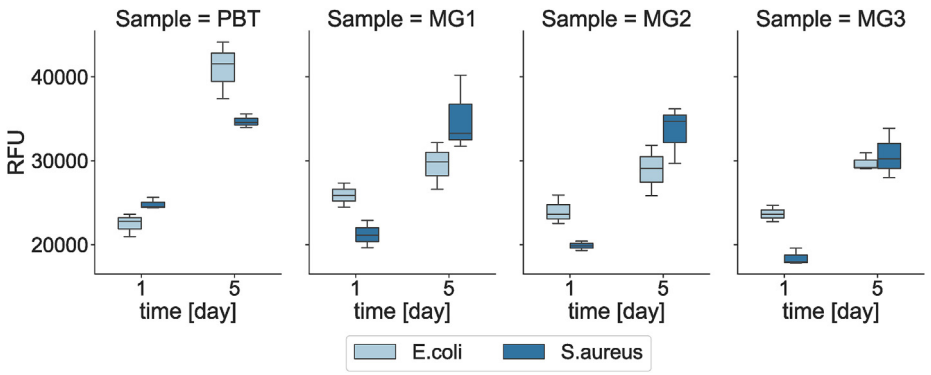

Fig. 8. Indirect antibacterial evaluation of PBT coated by Zr–Cu–Ag metallic glass coatings. Samples were incubated in LB (37 °C, 120 rpm) for 1day and 5days, and the supernatant was used to cultivate E.coli and S.aureus.

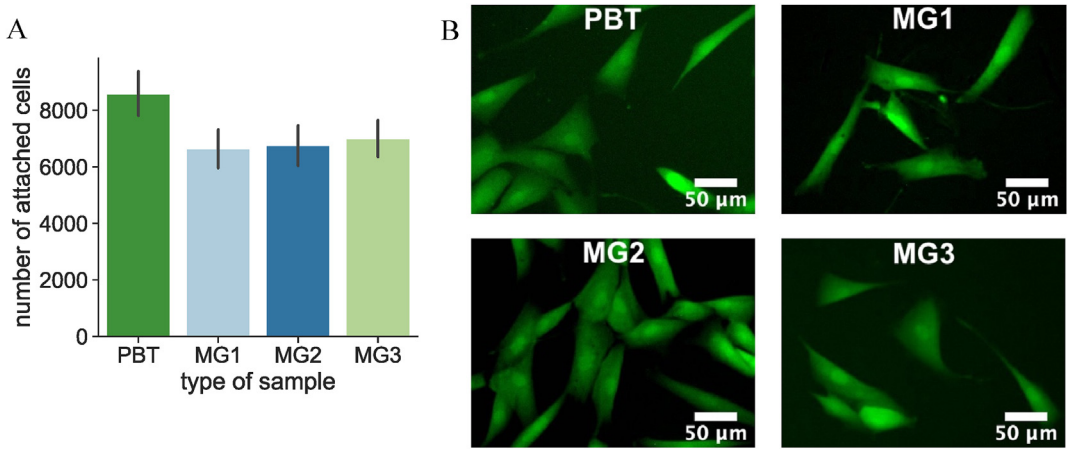

Fig. 9. Direct cytocompatibility evaluation of PBT coated by Zr–Cu–Ag metallic glass coatings. hMSC were cultivated directly on samples surface for 24 h, and the cytocompatibility was evaluated by: (A) number of attached hMSC on samples surface (B) Live/Dead images.

not significantly reduced in comparison to the control cells cultivated with ions-free PBT supernatants ($p > 0.05$). To explain these results, the ICP assay can be useful as the only ion clearly detectable (even after 5 days) was Cu, while Ag was detected in negligible amount. However, the maximum value detected for Cu was ≈120 ppb that in previous literature was considered as a low amount to induce antibacterial activity that requires at least 250 ppm to inactivate *S. aureus* [40]. This was demonstrated by Reyes-Jara et al. [40]; they have showed the copper MIC (Minimum inhibitory concentration) values between 375 and 700 ppm (that means these concentrations showed bacteriostatic properties; for bactericidal investigation, bacteria should be cultivated on solid agar plates); however, no bacterial growth was observed only at 1000 ppm. Therefore, this is a further confirmation that the good inhibitory data obtained from the not direct evaluation are mostly solely due to the antifouling properties ascribing to the superhydrophobic surfaces of the sputtered specimens and not to the coating chemical composition.

3.3. Cytocompatibility evaluation

3.3.1. Direct evaluation

Cytocompatibility of sputtered samples was *in vitro* preliminary investigated on hMSC cells. hMSC cells were directly cultured onto samples' surface and the numbers of attached cells were counted and presented in Fig. 9A while their metabolic assay was evaluated using fluorescent staining with Live/Dead Viability/Cytotoxicity staining and reported in Fig. 9B. PBT specimens were considered as 100% viability due to their known cells friendly properties [41].

According to the number of living attached cells on the samples' surfaces (Fig. 9A) and the live cells observed by fluorescent microscope (Fig. 9B), it can be concluded that the sputtered samples are not cytotoxic even after the ions doping. Moreover, FESEM images (Fig. 10) demonstrated how the cells were able to adhere and spread following the topography and orientation of the coating fibers that acted as guidance for the spread. These findings are in line with previous literature from the Authors showing that keratin microfibers were able to influence cells adhesion and spread over the roughness of the bulk material [28,42].

3.3.2. Not direct cytocompatibility evaluation

In line to the not direct assay evaluating released ions toxicity for bacteria, the same procedure was applied for cells. Here specimens were submerged with DMEM medium that was used to cultivate hMSC in a defined number (2×10^4/well) into 24 multiwell plates. After 1- and 5-days cultivation, the viability of the adhered cells was evaluated by metabolic alamar blue assay and visually confirmed by the fluorescent Live/Dead assay; results were compared to the ions-free PBT and then, the metal ions internalization was histologically investigated by means of the May-Grumwald-Giemsa specific staining. Results are summarized in Fig. 11.

In general, cells' metabolic activity resulted as comparable between the PBT control and the co-sputtered specimens after 24 h cultivation (Fig. 11A, $p > 0.05$); after 5 days cultivation, a general decrease of the metabolic activity was observed. However, the same trend was observed also for the ions-free PBT control, therefore speculating to the hypothesis that such reduction is not due to the sputtered ions but most probably to the low metabolic and phase reached by the cells after being 90% confluent to the reducing in nutrients in the 5-days old medium [41]. In fact, to prevent the ions removal form the medium, cells were maintained into the same medium for all the 5 days cultivation on the opposite to the typical

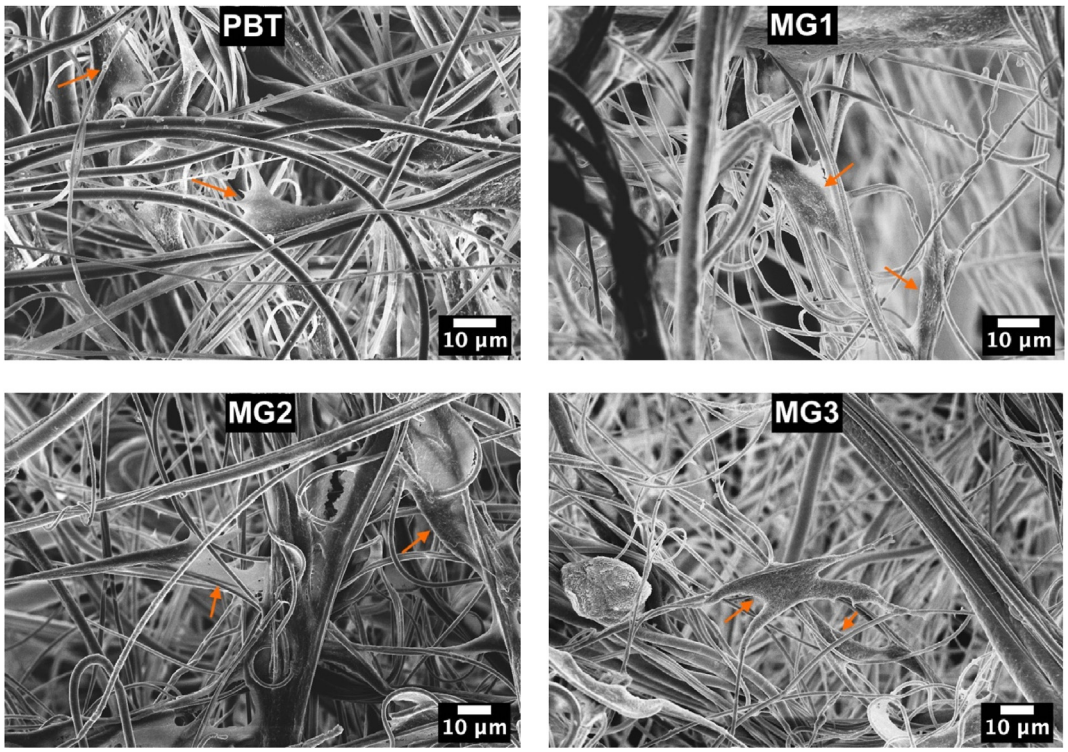

Fig. 10. FESEM images of samples after direct cytocompatibility evaluation. Figures show the attached hMSC on sample surfaces after 24 h.

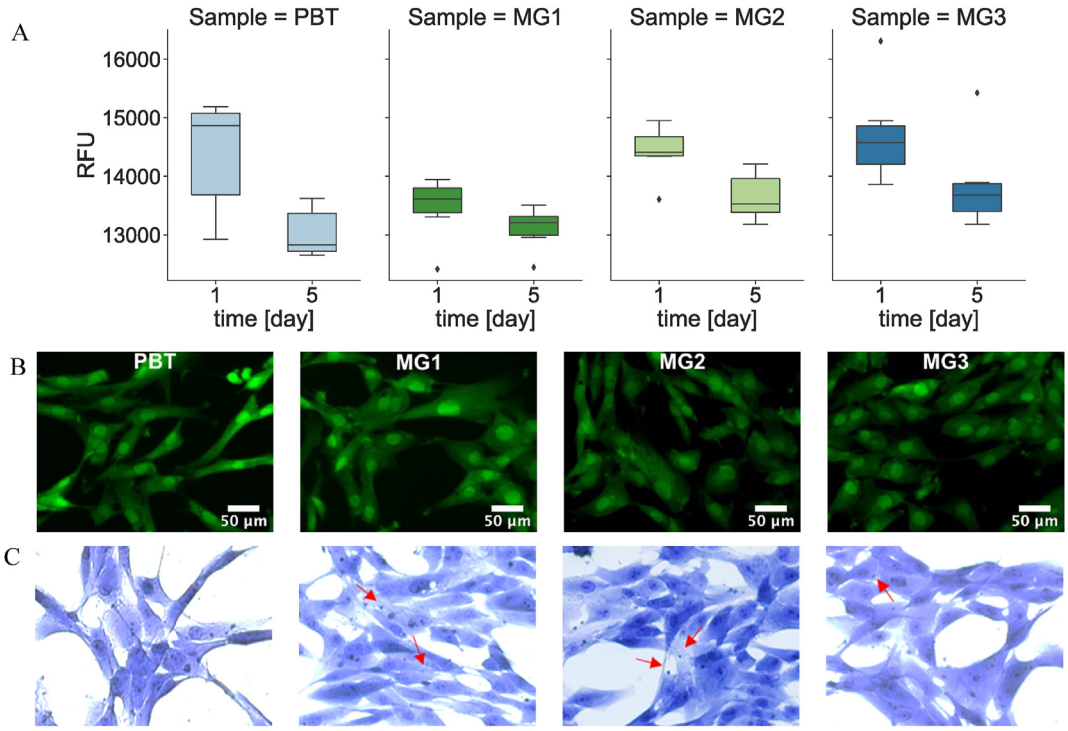

Fig. 11. Indirect cytocompatibility evaluation. (ion release approach). Samples were incubated in DMEM (37 °C, 120 rpm) for 1day and 5days, and the supernatant was used to cultivate hMSC in them A) Relative fluorescence unit (RFU) of BMSC B) Fluorescent staining by Live/Dead Viability/Cytotoxicity Kit after 5days, C) detection of ions inside the cells' cytoplasm with staining with May Grunwald and Giemsa after 5days.

change after 3 days. As a confirmation of the lack of toxicity, the Live/Dead (L/D) assay preformed onto cells cultivated for 5 days (Fig. 11B) demonstrated that cells cultivated with doped supernatants were mostly viable (stained in green); similarly, the May-Grumwald-Giemsa histology demonstrated that ions were internalized by cells (Fig. 11C, ions indicated by the red arrows) that previously demonstrated to be viable by the L/D assay previously performed. So, taken all together these data suggest that the ions sputtered into the specimens' coating did not introduced any toxic effect.

4. Conclusion

In this work, melt-blown Polybutylene terephthalate (PBT) fibrous textiles were coated to form an antifouling textile material. Metallic glass coatings based on co-sputtering Zr, Cu, and Ag on PBT surface with a range of chemical compositions were prepared. Small angle X-Ray scattering has confirmed the formation of amorphous structure of the coating. Sessile drop water contact angle measurement was conducted. It was shown that contact angle of water on PBT surface increases after coating and it turns the hydrophobic surface of PBT (CA = 124.5° ± 0.3) into superhydrophobic surface for some samples (MG3: static CA = 150.8° ± 0.1, and hysteresis = 3.5°). Among all prepared coatings, three samples with the static water contact angles of 130.8° ± 0.3, 143.6° ± 0.3, and 150.8° ± 0.1, and the chemical compositions of $Zr_{93.5}Cu_{6.2}Ag_{0.2}$, $Zr_{76.7}Cu_{22.7}Ag_{0.5}$, and $Zr_{69.3}Cu_{30.1}Ag_{0.6}$ respectively were selected to be further investigated for their antifouling properties. Sessile drop contact angle measurements were repeated on selected samples using LB and DMEM as liquid mediums. The same trend was observed for these mediums as the contact angle of LB and DMEM on PBT has increased after the coating. It was explained that the hydrophobicity of PBT could be attributed to the entrapment of air bubbles on its highly fibrous porous structure, observed under SEM. The excessive hydrophobicity after sputtering PBT surface is possibly related to the presence of metallic Zr on the surface. This observation was in line with several other reports related to contact angle measurements of Zr-based metallic glasses. To confirm the superhydrophobicity is samples, dynamic contact angle measurements (medium = water) were also performed on samples' surfaces and the hysteresis for each sample was obtained as a difference between advancing and receding angles. It was shown that the hysteresis of uncoated sample, PBT decreases from 15° to values below 10° for all coated samples. This in fact indicates a superhydrophobic surface for all three samples. The hysteresis values obtained for coated samples were measured to be 7.7°, 7.2°, and 3.5° for MG1, MG2, and MG3 respectively.

Ions released from coated samples into LB and DMEM solutions was measured by ICP-MS after 24 h and 5 days. It was shown that mainly copper is released into the solutions (≈50–120 ppb), and even in that case, its concentration is extremely below the toxic level for humans, and therefore, they pass the indirect cytocompatibility test. These results indicate that the non-wetting surface of the coating is responsible for antibacterial properties as ion-release from samples is extremely low.

Specimens' surfaces were infected with the Gram-positive *Staphylococcus aureus* and the Gram-negative *Escherichia coli* strain, they demonstrated a strong preventive antifouling property as ≈ 95% of the inoculated bacteria did not adhere into the surface determined by the count of the colony forming unit (CFU). Results were visually confirmed by FESEM images and fluorescent live/dead staining where only few viable single colonies were observed, thus excluding the formation of biofilm.

Direct cytocompatibility evaluation by human mesenchymal stem cells (hMSC) was conducted by cultivating them directly onto specimens' surface. hMSC were able to adhere and spread along coated fibers showing a metabolic activity comparable (≈90%) to those cultivated onto non-coated PBT therefore confirming for specimens cytocompatibility.

Author contribution

Elham Sharifikolouei: Conceptualization, Methodology, Writing – original draft, Funding acquisition, Ziba Najmi: Investigation, Writing – original draft, Andrea Cochis: Conceptualization, Methodology, Validation, Writing – review & editing, Alessandro Calogero Scalia: Investigation, Maryam Aliabadi: Investigation, Sergio Perero: Investigation, Lia Rimondini: Supervision, Resources, Validation

Declaration of competing interest

The authors declare that they have no known competing financial interests or personal relationships that could have appeared to influence the work reported in this paper.

Acknowledgments

We would like to thank European Commission for providing funding for this project under the Horizon 2020 research and innovation programme for Marie Skłodowska-Curie Individual Fellowship, with the acronym "MAGIC" and grant agreement N. 892050.

Appendix A. Supplementary data

Supplementary data to this article can be found online at https://doi.org/10.1016/j.mtbio.2021.100148.

References

[1] L.A. Herwaldt, J.J. Cullen, D. Scholz, P. French, M.B. Zimmerman, M.A. Pfaller, R.P. Wenzel, T.M. Perl, A prospective study of outcomes, healthcare Resource utilization, and costs associated with postoperative nosocomial infections, Infect. Control Hosp. Epidemiol. 27 (2006) 1291–1298, https://doi.org/10.1086/509827.

[2] A. Hanczvikkel, Á. Tóth, Quantitative study about the role of environmental conditions in the survival capability of multidrug-resistant bacteria, J. Infect. Public Health. 11 (2018) 801–806, https://doi.org/10.1016/j.jiph.2018.05.001.

[3] M. Katsikogianni, Y.F. Missirlis, L. Harris, J. Douglas, Concise review of mechanisms of bacterial adhesion to biomaterials and of techniques used in estimating bacteria-material interactions, Eur. Cell. Mater. 8 (2004) 37–57, https://doi.org/10.22203/eCM.v008a05.

[4] K. Ellinas, D. Kefallinou, K. Stamatakis, E. Gogolides, A. Tserepi, Is there a Threshold in the antibacterial action of superhydrophobic surfaces? ACS Appl. Mater. Interfaces 9 (2017) 39781–39789, https://doi.org/10.1021/ACSAMI.7B11402.

[5] S.M. Imani, R. Maclachlan, K. Rachwalski, Y. Chan, B. Lee, M. McInnes, K. Grandfield, E.D. Brown, T.F. Didar, L. Soleymani, Flexible hierarchical wraps Repel drug-resistant gram-negative and positive bacteria, ACS Nano 14 (2020) 454–465, https://doi.org/10.1021/acsnano.9b06287.

[6] W. Ma, Y. Li, M. Zhang, S. Gao, J. Cui, C. Huang, G. Fu, Biomimetic durable multifunctional self-cleaning nanofibrous membrane with outstanding oil/water separation, photodegradation of organic Contaminants, and antibacterial performances, ACS Appl. Mater. Interfaces 12 (2020) 34999–35010, https://doi.org/10.1021/acsami.0c09059.

[7] W. Ma, Y. Ding, Y. Li, S. Gao, Z. Jiang, J. Cui, C. Huang, G. Fu, Durable, self-healing superhydrophobic nanofibrous membrane with self-cleaning ability for highly-efficient oily wastewater purification, J. Membr. Sci. 634 (2021) 119402, https://doi.org/10.1016/j.memsci.2021.119402.

[8] T. Lu, Y. Deng, J. Cui, W. Cao, Q. Qu, Y. Wang, R. Xiong, W. Ma, J. Lei, C. Huang, Multifunctional applications of blow-spinning Setaria viridis structured fibrous membranes in water purification, ACS Appl. Mater. Interfaces 13 (2021) 22874–22883, https://doi.org/10.1021/acsami.1c05667.

[9] M. Zhang, J. Cui, T. Lu, G. Tang, S. Wu, W. Ma, C. Huang, Robust, functionalized reduced graphene-based nanofibrous membrane for contaminated water purification, Chem. Eng. J. 404 (2021) 126347, https://doi.org/10.1016/j.cej.2020.126347.

[10] A. Zhou, Y. Zhang, Q. Qu, F. Li, T. Lu, K. Liu, C. Huang, Well-defined multifunctional superhydrophobic green nanofiber membrane based-polyurethane with inherent antifouling, antiadhesive and photothermal bactericidal properties and its application in bacteria, living cells and zebra fish, Compos. Commun. 26 (2021) 100758, https://doi.org/10.1016/J.COCO.2021.100758.

[11] N. Beyth, Y. Houri-Haddad, A. Domb, W. Khan, R. Hazan, Alternative antimicrobial approach: nano-antimicrobial materials, evidence-based complement, Altern. Med. 2015 (2015), https://doi.org/10.1155/2015/246012.

[12] I. Sondi, B. Salopek-Sondi, Silver nanoparticles as antimicrobial agent: a case study on E. coli as a model for Gram-negative bacteria, J. Colloid Interface Sci. 275 (2004) 177–182, https://doi.org/10.1016/j.jcis.2004.02.012.

[13] W.R. Li, X.B. Xie, Q.S. Shi, H.Y. Zeng, Y.S. Ou-Yang, Y. Ben Chen, Antibacterial activity and mechanism of silver nanoparticles on Escherichia coli, Appl. Microbiol. Biotechnol. 85 (2010) 1115–1122, https://doi.org/10.1007/s00253-009-2159-5.

[14] S. Ferraris, S. Perero, P. Costa, G. Gautier di Confiengo, A. Cochis, L. Rimondini, F. Renaux, E. Vernè, M. Ferraris, S. Spriano, Antibacterial inorganic coatings on metallic surfaces for temporary fixation devices, Appl. Surf. Sci. 508 (2020) 144707, https://doi.org/10.1016/j.apsusc.2019.144707.

[15] G. Grass, C. Rensing, M. Solioz, Metallic copper as an antimicrobial surface, Appl. Environ. Microbiol. 77 (2011) 1541–1547, https://doi.org/10.1128/AEM.02766-10.

[16] D.C. Ford, D. Hicks, C. Oses, C. Toher, S. Curtarolo, Metallic glasses for biodegradable implants, Acta Mater. 176 (2019) 297–305, https://doi.org/10.1016/j.actamat.2019.07.008.
[17] C.S.S. Zr-based, Facile Electrochemical Method for the Fabrication of Stable, 2021.
[18] S. Xiao, H. Zhang, S. Guo, Fabrication of a Zr-based bulk metallic glass surface with extreme wettability, J. Non-Cryst. Solids 536 (2020) 120001, https://doi.org/10.1016/j.jnoncrysol.2020.120001.
[19] N. Li, T. Xia, L. Heng, L. Liu, Superhydrophobic Zr-based metallic glass surface with high adhesive force, Appl. Phys. Lett. 102 (2013) 251603, https://doi.org/10.1063/1.4812480.
[20] N. Lin, P. Berton, C. Moraes, R.D. Rogers, N. Tufenkji, Nanodarts, nanoblades, and nanospikes: mechano-bactericidal nanostructures and where to find them, Adv. Colloid Interface Sci. 252 (2018) 55–68, https://doi.org/10.1016/j.cis.2017.12.007.
[21] Y. Liu, J. Padmanabhan, B. Cheung, J. Liu, Z. Chen, B.E. Scanley, D. Wesolowski, M. Pressley, C.C. Broadbridge, S. Altman, U.D. Schwarz, T.R. Kyriakides, J. Schroers, Combinatorial development of antibacterial Zr-Cu-Al-Ag thin film metallic glasses, Sci. Rep. 6 (2016) 1–8, https://doi.org/10.1038/srep26950.
[22] G.I. Nkou Bouala, A. Etiemble, C. Der Loughian, C. Langlois, J.F. Pierson, P. Steyer, Silver influence on the antibacterial activity of multi-functional Zr-Cu based thin film metallic glasses, Surf. Coating. Technol. 343 (2018) 108–114, https://doi.org/10.1016/j.surfcoat.2017.10.057.
[23] P. Yiu, W. Diyatmika, N. Bönninghoff, Thin film metallic glasses: properties, applications and future ARTICLES YOU MAY BE INTERESTED IN, J. Appl. Phys. 127 (2020) 30901, https://doi.org/10.1063/1.5122884.
[24] T. Çaykara, M.G. Sande, N. Azoia, L.R. Rodrigues, C.J. Silva, Exploring the potential of polyethylene terephthalate in the design of antibacterial surfaces, Med. Microbiol. Immunol. 209 (2020) 363–372, https://doi.org/10.1007/s00430-020-00660-8.
[25] P.A. Ramires, L. Mirenghi, A.R. Romano, F. Palumbo, G. Nicolardi, Plasma-treated PET surfaces improve the biocompatibility of human endothelial cells, J. Biomed. Mater. Res. 51 (2000) 535–539, https://doi.org/10.1002/1097-4636(20000905)51:3<535::AID-JBM31>3.0.CO;2-P.
[26] L.W. McKeen, Polyesters, eff. Long term Therm. Expo, Plast. Elastomers. (2014) 85–115, https://doi.org/10.1016/B978-0-323-22108-5.00005-9.
[27] N.P. Cheremisinoff, P, Condens. Encycl. Polym. Eng. Terms (2001) 200–255, https://doi.org/10.1016/B978-0-08-050282-3.50021-4.
[28] A. Cochis, S. Ferraris, R. Sorrentino, B. Azzimonti, C. Novara, F. Geobaldo, F. Truffa Giachet, C. Vineis, A. Varesano, A. Sayed Abdelgeliel, S. Spriano, L. Rimondini, Silver-doped keratin nanofibers preserve a titanium surface from biofilm contamination and favor soft-tissue healing, J. Mater. Chem. B. 5 (2017) 8366–8377, https://doi.org/10.1039/c7tb01965c.
[29] S. Ferraris, A. Cochis, M. Cazzola, M. Tortello, A. Scalia, S. Spriano, L. Rimondini, Cytocompatible and anti-bacterial adhesion nanotextured titanium Oxide layer on titanium surfaces for dental and orthopedic implants, Front. Bioeng. Biotechnol. 7 (2019) 103, https://doi.org/10.3389/fbioe.2019.00103.
[30] D. Wojcieszak, M. Osekowska, D. Kaczmarek, B. Szponar, M. Mazur, P. Mazur, A. Obstarczyk, Influence of material composition on structure, surface properties and biological activity of nanocrystalline coatings based on Cu and Ti, Coatings 10 (2020) 343, https://doi.org/10.3390/coatings10040343.
[31] V.M. Villapún, H. Zhang, C. Howden, L.C. Chow, F. Esat, P. Pérez, J. Sort, S. Bull, J. Stach, S. González, Antimicrobial and wear performance of Cu-Zr-Al metallic glass composites, Mater. Des. 115 (2017) 93–102, https://doi.org/10.1016/j.matdes.2016.11.029.
[32] P. Zeman, M. Zítek, Zuzjaková, R. Čerstvý, Amorphous Zr-Cu thin-film alloys with metallic glass behavior, J. Alloys Compd. 696 (2017) 1298–1306, https://doi.org/10.1016/j.jallcom.2016.12.098.
[33] C.J. van Oss, R.F. Giese, A. Docoslis, Hyperhydrophobicity of the water-air interface, J. Dispersion Sci. Technol. 26 (2005) 585–590, https://doi.org/10.1081/DIS-200057645.
[34] C.R. Crick, S. Ismail, J. Pratten, I.P. Parkin, An investigation into bacterial attachment to an elastomeric superhydrophobic surface prepared via aerosol assisted deposition, Thin Solid Films 519 (2011) 3722–3727, https://doi.org/10.1016/j.tsf.2011.01.282.
[35] A. Cochis, B. Azzimonti, C. Della Valle, E. De Giglio, N. Bloise, L. Visai, S. Cometa, L. Rimondini, R. Chiesa, The effect of silver or gallium doped titanium against the multidrug resistant Acinetobacter baumannii, Biomaterials 80 (2016) 80–95, https://doi.org/10.1016/j.biomaterials.2015.11.042.
[36] X. Zhang, L. Wang, E. Levänen, Superhydrophobic surfaces for the reduction of bacterial adhesion, RSC Adv. 3 (2013) 12003–12020, https://doi.org/10.1039/c3ra40497h.
[37] C.P. Stallard, K.A. McDonnell, O.D. Onayemi, J.P. O'Gara, D.P. Dowling, Evaluation of protein adsorption on atmospheric plasma deposited coatings exhibiting superhydrophilic to superhydrophobic properties, Biointerphases 7 (2012) 1–12, https://doi.org/10.1007/s13758-012-0031-0.
[38] W. Barthlott, C. Neinhuis, Purity of the sacred lotus, or escape from contamination in biological surfaces, Planta 202 (1997) 1–8, https://doi.org/10.1007/s004250050096.
[39] B.J. Privett, J. Youn, S.A. Hong, J. Lee, J. Han, J.H. Shin, M.H. Schoenfisch, Antibacterial fluorinated silica colloid superhydrophobic surfaces, Langmuir 27 (2011) 9597–9601, https://doi.org/10.1021/la201801e.
[40] A. Reyes-Jara, N. Cordero, J. Aguirre, M. Troncoso, G. Figueroa, Antibacterial effect of copper on microorganisms isolated from bovine mastitis, Front. Microbiol. 7 (2016) 626, https://doi.org/10.3389/fmicb.2016.00626.
[41] B.V.M. Rodrigues, A.S. Silva, G.F.S. Melo, L.M.R. Vasconscellos, F.R. Marciano, A.O. Lobo, Influence of low contents of superhydrophilic MWCNT on the properties and cell viability of electrospun poly (butylene adipate-co-terephthalate) fibers, Mater. Sci. Eng. C 59 (2016) 782–791, https://doi.org/10.1016/j.msec.2015.10.075.
[42] S. Ferraris, F. Truffa Giachet, M. Miola, E. Bertone, A. Varesano, C. Vineis, A. Cochis, R. Sorrentino, L. Rimondini, S. Spriano, Nanogrooves and keratin nanofibers on titanium surfaces aimed at driving gingival fibroblasts alignment and proliferation without increasing bacterial adhesion, Mater. Sci. Eng. C 76 (2017) 1–12, https://doi.org/10.1016/j.msec.2017.02.152.